Research Article

Design of Wavelength Selectively Metamaterial Antenna for Thermal Camouflage

Atıf Kerem Şanlı[1*], Timuçin Emre Tabaru[2,3,4] and Veli Tayfun Kılıç[5]

[1]*Dept. of Electrical and Electronics Engineering, Orcid ID: 0000-0001-8304-8154, Abdullah Gul University., 38039, Kayseri, Turkey*
[2]*Department of Electrical-Electronic Engineering, Orcid ID: 0000-0002-1373-3620 Sivas University of Science and Technology, Sivas 58010, Turkey*
[3]*UNAM-Institute of Materials Science and Nanotechnology, Bilkent University, Ankara 06800, Turkey*
[4]*Department of Clinical Engineering Research and Application Center, Erciyes University, Kayseri 38039, Turkey*
[5]*Dept. of Electrical and Electronics Engineering, Orcid ID: 0000-0001-6806-9053, Abdullah Gul University., 38039, Kayseri, Turkey*

[*]Correspondence: atif.sanli@agu.edu.tr;

(First received September 14, 2022 and in final form December 19, 2022)

Reference: Şanlı A. K., Tabaru T. E., Kılıç, V. T. Design of Wavelength Selectively Metamaterial Antenna for Thermal Camouflage. The European Journal of Research and Development,2(4), 90-97.

Abstract

Phase transition materials offer exciting opportunities to dynamically control the optical properties of photonic devices. As a special phase change material (PCM), vanadium dioxide (VO_2) is an excellent alternative for thermal camouflage technology research. Due to the unique property of VO_2, coupled with the metallic structure can enable the design of thermally reconfigurable absorbers that allow resonance tuning. We propose a very simple, multi-layered with metamaterial excellent thermal emitter nanoantenna. The size of our design is only 1365 nm for the infrared wavelength range from 0.8 to 12 µm. Concept silver (Ag), VO_2, dielectric separator and silver (Ag) configuration are used for finite difference time domain (FDTD) analysis. The absorption band can be further expanded with more deposition layers with various metals. In this paper, a thermal camouflage mid-infrared adaptive metamaterial antenna based on a PCM metamaterial is designed to fit perfectly into atmospheric windows. The spectral properties of the structure were calculated using FDTD method. The distinctive feature of the proposed structure is that adaptations can be made by placing an ultra-thin VO_2 interlayer between the metallic structures. We believe that the proposed design is very promising in terms of simple fabrication and modifiable aspects for wide-area broadband unity absorption.

Keywords: Phase change material, Vanadium dioxide, Thermal camouflage technology, Metamaterial, Thermal emitter nanoantenna.

1. Introduction

Thermal camouflage technology is a study that ensures that objects (individuals, warplanes, navy ships, tanks, etc.) that leaves thermal traces by emitting heat are invisible to threats from thermal cameras, heat-seeking missiles, or other thermal detection equipment, thus preventing them from being targeted [1 -3]. It's basic working principle is based on Plank's Law. According to Plank's law, objects that are not at absolute zero temperature, which is -273.15 °C, continue to radiate heat to the outside environment [4]. Because of this radiated heat, their thermal traces can be detected, so they can be targeted. The temperature of the human body has been found to be 37°C in ideal conditions, engines of fighter jets around 700°C [5], navy ships and airplane exhaust pipes around 450°C [6,7]. It is easy to detect objects with these values by thermal scanning systems and then they can become targets. For these reasons, thermal camouflage technology is urgently demanded. The heat emitted by objects above absolute zero occurs mostly in the mid-infrared region (5-40 μm [8]) and in the near-infrared region (0.7-5 μm [8]). The provision of thermal camouflage on heat radiating objects can be achieved by controlling the radiated heat emission in these spectral regions. For this purpose, many different meta-materials or structures such as films have been designed at the nanoscale. With the help of these structures, the heat emission of the object to be protected can be moved outside the working spectrum of the thermal scanning devices or to the non-transmissive region (5-8 μm [9-14]), or the structure can absorb this heat. In this way, the targets can be protected by making them invisible.

In this study, a nano-sized metamaterial with a VO_2 film that emits at selective wavelengths in the non-transmissive region is presented. With its impressive properties and behavior, VO_2 offers a significant broadening of resonance peaks, especially in the non-transmissive region. In this way, it is possible to expand the invisibility spectrum of the targeted object. The 1516 nm narrow band resonance peak and the 6724 nm wide band resonance peak we obtained in the simulations performed at 363 K; In addition, the narrow band resonance peaks at 1513 and 2192 nm and the broad band resonance peak at 6422 nm, which is performed at 300 K, perfectly match the conditions of the spectral regions mentioned above.

2. Materials and Methods

The three-dimensional design of the presented nanostructure is shown in Figure 1. Numerical calculations were conducted within the design and simulations with a commercial finite difference time domain (FDTD) software. Within the structure, there are two silver (Ag) layers, the nanostructure, and the lower substrate, with refractive index data taken from the CRC Handbook of Chemistry and Physics [15]. Between the Ag layers, there is a dielectric layer with a refractive index of 1.46 and VO_2. The simulation temperature was determined as 363 K (90 °C) and 300 K (25 °C), respectively, in order to better observe the phase change (metal and insulator) properties of VO_2. The spectral region of 0.8 - 12 μm, located in the infrared region, was chosen as the source, and illuminated in the backward "z" direction ("-z") with a regular planar wave. The thicknesses of the materials used in the design in the "z" direction, from top to bottom, are as follows:

- Upper Ag layer (t_{Ag}): 160 nm,
- VO_2 layer (t_{VO2}): 5 nm,
- Dielectric layer (t_D): 15 nm,
- Sub-Ag layer (t_{SUB}): 100 nm.

The boundary conditions of the simulation were determined periodically along the "x" and "y" axes. The period is 1365 nm and the width values of the materials are determined as follows:

- Upper Ag layer (W_{Ag}): 1100 nm,
- VO_2 layer (W_{VO2}): 1100 nm,
- Dielectric layer: 1365 nm,
- Sub-Ag layer (substrate): 1365 nm

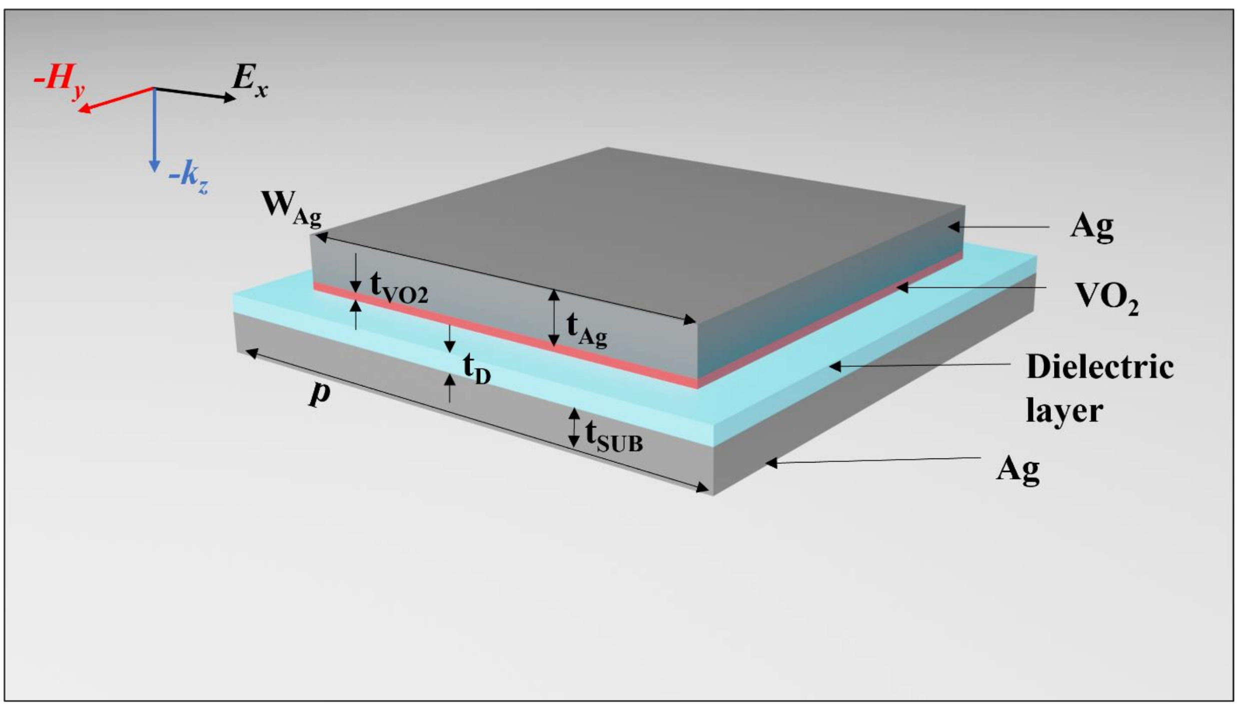

Figure 1: *3D Design of nanoantenna.*

3. Results

VO_2 is a material that behaves differently depending on the temperature it is exposed to. VO_2 shows two different modes above and below the critical threshold of 68 °C. One of these modes is known as insulator mode below 68 °C and metal mode above [16]. And in Figure 2, the refractive indices of the materials belonging to these two modes are given. Thanks to this phase change material, it can be used to provide thermal camouflage for an individual with a body temperature of 37 ˚C or to hide a fighter jet engine operating at 700 °C, without the need for redesigns. The absorption values of VO_2, which can act as a metal and insulator, at 90 °C and 27 °C are shown in Figure 4 within the spectrum including the atmospheric non-transmissive region between 5-8 µm.

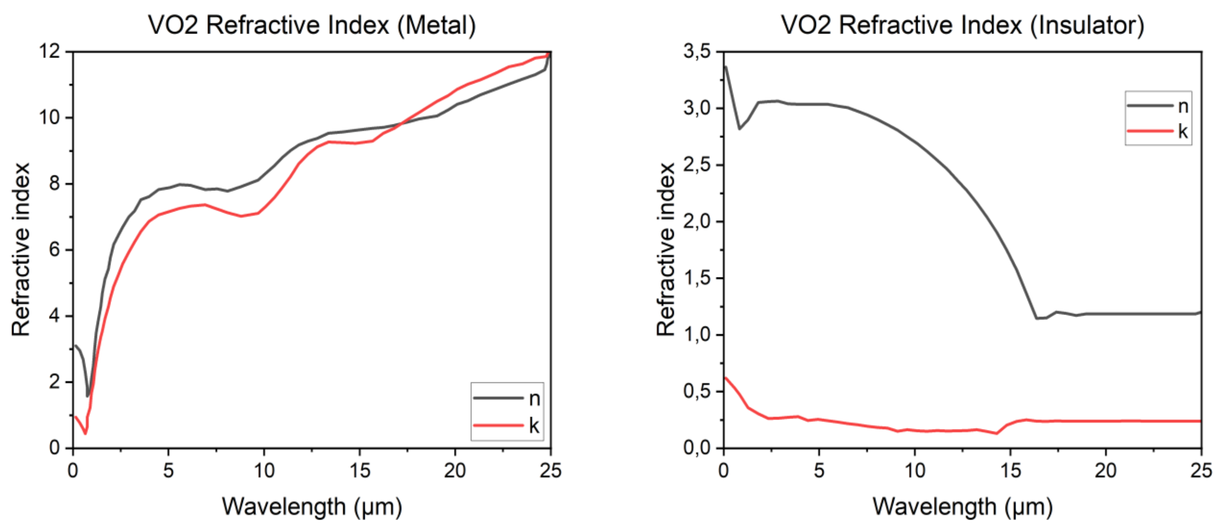

Figure 2: *VO_2 refractive indices of metal and insulator mods. [16]*

Figures 3 and 4 show the absorption values of the proposed metamaterial antenna at 300 K (insulator mode) and 363 K (metal mode), respectively, depending on wavelength. Temperature is the main cause of the change in resonance peaks. In addition, it has been observed that the width, height, briefly the geometrical characteristics of the layers inside the structure can also affect the absorption.

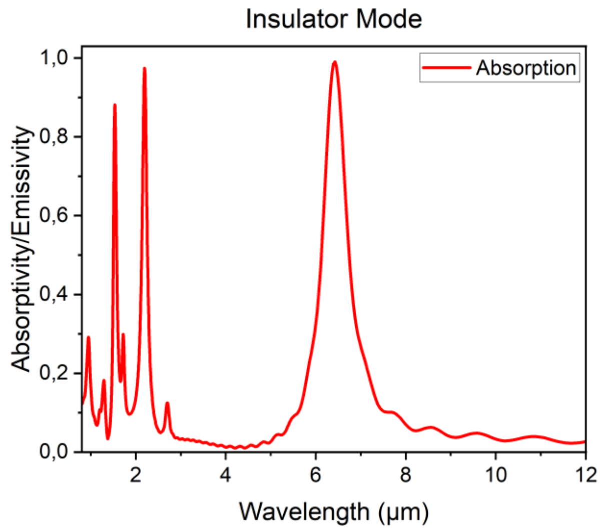

Figure 3: *Thermal absorption graph of purposed metamaterial antenna at 300K temperature.*

In Figure 3, VO_2 at 300 K was acting in insulator mode, while the presented metamaterial antenna showed two narrow band resonance peaks, first at emissivity (ε) = 0.88 with a peak at 1513 nm and then at ε = 0.97 with a peak at 2192 nm. In the insulator mode, a broadband resonance peak was observed at ε = 0.99 with a peak of 6422 nm in the non-transmissive region.

In Figure 4, as a result of the simulations, the presented metamaterial antenna behaved in the VO_2 metal mode at 363 K, and firstly showed a narrow band resonance peak reaching almost the maximum absorption at ε = 0.98 at 1516 nm. In following atmospheric non-transmissive region, a broad band resonance peak which is at 6724 nm with ε = 0.89 in the non-transmissive region, which is the critical region for thermal camouflage and the region between 5-8μm where absorption reaches its maximum.

In Figure 5, the absorption data obtained in metal and insulator modes, while the presented metamaterial antenna with VO_2 layer is operating at 363 K and 300 K, is intertwined with data representing atmospheric absorption values.

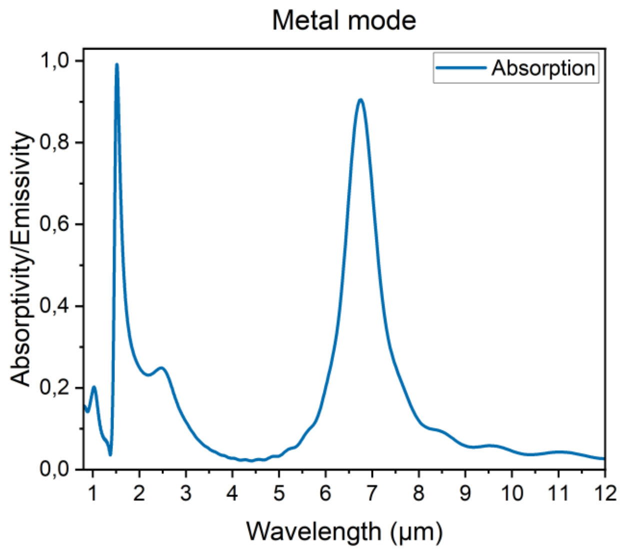

Figure 4: *Thermal absorption graph of purposed metamaterial antenna at 363K temperature.*

In addition to broadband absorption in the non-transmissive region, the metamaterial antenna also showed high absorption narrow band resonance peaks in the non-transmissive region between 1.4–1.9 µm and broad band resonance peaks in the non-transmissive region between 5–8 µm.

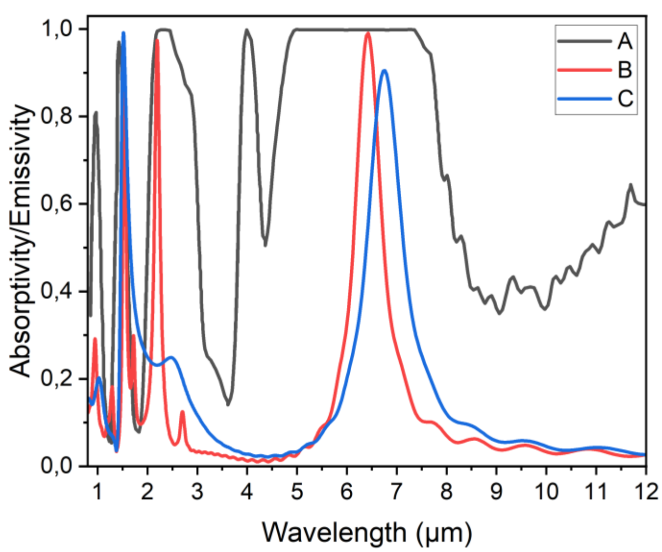

Figure 5: *The simulated incidence Absorptivity/Emissivity spectrum. A: Atmospheric transmissive/non-transmissive window, B: Purposed metamaterial antenna for VO_2 insulator mode, C: Purposed metamaterial antenna for VO_2 metal mode.*

4. Discussion and Conclusion

As conclusion, in this study, we present a multilayer absorber metamaterial consisting of VO_2, Ag and dielectric layers. Besides, it has dual absorptivity/emissivity resonance peaks. VO_2 was analyzed numerically together with the dielectric layer between the metal Ag layers and the temperature-dependent changes were visualized in the relevant spectral regions. The width and depth of the resonance peaks, in addition to being directly affected by the temperature-dependent behavior of VO_2, also vary depending on the height and width of the layers in the structure, the boundary conditions in which the experiment is conducted, and the periodicity. In the further stages of the research, it is aimed to include all resonance values in the atmospheric absorption area and to further expand the resonance peaks in the non-transmissive region. As can be seen from the obtained data, it has been observed that the designed metamaterial antenna has high absorption peaks in the atmospheric non-transmissive region. A situation has been presented where the absorption values of the determined peaks approached the unit value, and therefore, thermal detectors could not detect it. Therefore, it has been presented that the designed metamaterial antenna can be used with high performance and efficiency in thermal camouflage applications in defense technologies.

5. Acknowledge

We would like to thank Ekmel Özbay and Ataollah Kalantari Osgouei for their support during the research.

References

[1] Baranwal, N., & Mahulikar, S. P. (2016). Infrared signature of aircraft engine with choked converging nozzle. Journal of thermophysics and heat transfer, 30(4), 854-862.

[2] Karshalev, E. (2020). Materials and Designs for Small-Scale Propelled Devices Towards Environmental and Biological Applications. University of California, San Diego.

[3] Xie, X., Li, X., Pu, M., Ma, X., Liu, K., Guo, Y., & Luo, X. (2018). Plasmonic metasurfaces for simultaneous thermal infrared invisibility and holographic illusion. Advanced Functional Materials, 28(14), 1706673.

[4] Baranov, D. G., Xiao, Y., Nechepurenko, I. A., Krasnok, A., Alù, A., & Kats, M. A. (2019). Nanophotonic engineering of far-field thermal emitters. Nature materials, 18(9), 920-930.

[5] Mahulikar, S. P., Rao, G. A., & Kolhe, P. S. (2006). Infrared signatures of low-flying aircraft and their rear fuselage skin's emissivity optimization. Journal of Aircraft, 43(1), 226-232.

[6] Thompson, J., Vaitekunas, D., & Birk, A. M. (1998, January). IR signature suppression of modern naval ships. In ASNE 21st century combatant technology symposium (Vol. 1, pp. 27-30).

[7] Zhu, H., Li, Q., Tao, C., Hong, Y., Xu, Z., Shen, W., ... & Qiu, M. (2021). Multispectral camouflage for infrared, visible, lasers and microwave with radiative cooling. Nature communications, 12(1), 1-8.

[8] INFRARED PROCESSING AND ANALYSIS CENTER. Near, mid & far infrared. https://www.icc.dur.ac.uk/~tt/Lectures/Galaxies/Images/Infrared/Regions/irregions.html. Last access: November 16, 2022.

[9] Feng, X., Xie, X., Pu, M., Ma, X., Guo, Y., Li, X., & Luo, X. (2020). Hierarchical metamaterials for laser-infrared-microwave compatible camouflage. Optics express, 28(7), 9445-9453.

[10] Qu, Y., Li, Q., Cai, L., Pan, M., Ghosh, P., Du, K., & Qiu, M. (2018). Thermal camouflage based on the phase-changing material GST. Light: Science & Applications, 7(1), 1-10.

[11] Kim, T., Bae, J. Y., Lee, N., & Cho, H. H. (2019). Hierarchical metamaterials for multispectral camouflage of infrared and microwaves. Advanced Functional Materials, 29(10), 1807319.

[12] Pan, M., Huang, Y., Li, Q., Luo, H., Zhu, H., Kaur, S., & Qiu, M. (2020). Multi-band middle-infrared-compatible camouflage with thermal management via simple photonic structures. Nano Energy, 69, 104449.

[13] Peng, L., Liu, D., Cheng, H., Zhou, S., & Zu, M. (2018). A multilayer film based selective thermal emitter for infrared stealth technology. Advanced Optical Materials, 6(23), 1801006.

[14] Osgouei, A. K., Buhara, E., Khalichi, B., Ghobadi, A., & Ozbay, E. (2021, October). Wavelength selectivity in a polarization-insensitive metamaterial-based absorber consistent with atmospheric absorption windows. In 2021 IEEE Photonics Conference (IPC) (pp. 1-2). IEEE.

[15] Lide, D. R. (2004). CRC Handbook of Chemistry and Physics, 84th. Electrochemical Series. CRC Press LLC.

[16] Beaini, R., Baloukas, B., Loquai, S., Klemberg-Sapieha, J. E., & Martinu, L. (2020). Thermochromic VO_2-based smart radiator devices with ultralow refractive index cavities for increased performance. Solar Energy Materials and Solar Cells, 205, 110260.